

# Differentially Private Data Generation Needs Better Features

**Frederik Harder**  
MPI-IS & University of Tübingen  
fharder@tue.mpg.de

**Milad Jalali Asadabadi**  
UBC  
miladj7@cs.ubc.ca

**Danica J. Sutherland**  
UBC & Amii  
dsuth@cs.ubc.ca

**Mijung Park**  
UBC & Amii  
mijungp@cs.ubc.ca

## Abstract

Training even moderately-sized generative models with differentially-private stochastic gradient descent (DP-SGD) is difficult: the required level of noise for reasonable levels of privacy is simply too large. We advocate instead building off a good, relevant representation on public data, then using private data only for “transfer learning.” In particular, we minimize the maximum mean discrepancy (MMD) between private target data and the generated distribution, using a kernel based on perceptual features from a public dataset. With the MMD, we can simply privatize the data-dependent term once and for all, rather than introducing noise at each step of optimization as in DP-SGD. Our algorithm allows us to generate CIFAR10-level images faithfully with  $\epsilon \approx 2$ , far surpassing the current state of the art, which only models MNIST and FashionMNIST at  $\epsilon \approx 10$ . Our work introduces simple yet powerful foundations for reducing the gap between private and non-private deep generative models.

## 1 Introduction

The gold standard privacy notion, *differential privacy* (DP), is now ubiquitous in a diverse range of academic research, industry products [41], and even government databases [29]. DP provides a mathematically provable privacy guarantee, which is its main strength and reason for its popularity. However, one of the properties of DP is *composability*, meaning data can be accessed more than once – but the level of privacy guarantee degrades each time. To guarantee a high level of privacy, one needs to limit access to data, a challenge in applying DP with the usual iterative optimization algorithms used in machine learning.

Differentially private data generation solves this problem by creating a synthetic dataset that is *similar* to the private dataset, in terms of some chosen similarity metric. While producing such a synthetic dataset incurs a privacy loss, the resulting dataset can be used repeatedly without further loss of privacy. Classical approaches, however, typically assume a certain class of pre-specified purposes on how the synthetic data can be used [16, 27, 46, 52]. If data analysts use the data for other tasks outside these pre-specified purposes, the theoretical guarantees on its utility are lost.

To produce synthetic data usable for potentially *any* purpose, many papers on DP data generation have utilized the recent advances in deep generative modelling. The majority of these approaches are based on the generative adversarial network (GAN) [13] framework, where a discriminator and a generator play an adversarial game to optimize a given distance metric between the true and synthetic data distributions. Most approaches under this framework have used DP-SGD [1], where the gradients of the discriminator (which compares generated samples to private data) are privatized in each training

step, resulting in a high overall privacy loss [12, 31, 42, 48, 49]. Another challenge is that, as the gradients must have bounded norm to derive the DP guarantee, the amount of noise for privatization in DP-SGD increases proportionally to the dimension of the discriminator. Hence, these methods are typically bound to relatively small discriminators, limiting the ability to learn data distributions beyond, say, MNIST [23] or FashionMNIST [45].

Given these challenges, the heavy machinery such as GANs and large-scale auto-encoder-based methods – capable of generating complex datasets in a non-private setting – fails to model datasets such as CIFAR-10 [20] or CelebA [26] with a meaningful privacy guarantee (e.g.,  $\epsilon \approx 2$ ). These are datasets which typical deep generative modeling papers have moved well beyond, but currently there is no DP data generation method that can produce reliable samples at a reasonable privacy level.

How can we reduce this huge gap between the performance of non-private deep generative models and that of private counterparts? We argue that the solution to narrow down this gap lies in the employing abundant, resourceful public data. Our reasoning is in line with the core message of Tramer and Boneh [43]: *We simply need better features for differentially private learning*. While Tramer and Boneh demonstrated this reasoning in the context of DP classification, we aim to show the validity of this reasoning in the context of (more challenging) DP data generation, with a focus on high-dimensional image generation.

We propose to exploit public data to learn *perceptual features* (PFs) from public data, which we will use to compare synthetic and real data distributions. Following [9], we use “perceptual features” to mean the vector of all activations of a pretrained deep network for a given data point, e.g. the hundreds of thousands of hidden activations from applying a trained ResNet classifier to an image. Building on [9] that utilizes PFs for transfer learning in natural image generation, our goal is to utilize those to improve the quality of natural images generated with differential privacy constraints.

In our method, we construct a kernel on images using these powerful PFs, then train a generator by minimizing the Maximum Mean Discrepancy (MMD) [14] with that kernel between distributions [as in 4, 9, 11, 15, 24]. Compared to existing DP-GAN frameworks, this scheme is non-adversarial, leading to simpler and more stable optimization; more importantly, it allows us to privatize the mean embedding of the private dataset *once*, then use it at each step of generator training without incurring cumulative privacy losses.

We observe in our experiments that as long as the public data contains more complex patterns than private data, e.g., transferring the knowledge learned from ImageNet as public data to generate CIFAR-10 images as private data, the learned features from public data are useful enough to generate good synthetic data. We successfully generate reasonable samples for CIFAR-10, CelebA, MNIST, and FashionMNIST in high-privacy regimes. We also theoretically analyze the effect of privatizing our loss function, helping understand the privacy-accuracy trade-offs in our method.

## 2 Background

**Maximum Mean Discrepancy** The MMD is a distance between distributions corresponding to a kernel  $k(x, y) = \langle \phi(x), \phi(y) \rangle_{\mathcal{H}}$ , where  $\phi$  maps our data domain  $\mathcal{X}$  to a Hilbert space  $\mathcal{H}$ . One of several equivalent definitions [14] is:  $\text{MMD}(P, Q) = \|\mathbb{E}_{x \sim P}[\phi(x)] - \mathbb{E}_{y \sim Q}[\phi(y)]\|_{\mathcal{H}}$ , where  $\mathbb{E}_{x \sim P}[\phi(x)] \in \mathcal{H}$  is known as the (kernel) *mean embedding* of  $P$ , and is guaranteed to exist if  $\mathbb{E}_{x \sim P} \sqrt{k(x, x)} < \infty$  [38]. If  $k$  is *characteristic* [40], then  $P \mapsto \mathbb{E}_{x \sim P}[\phi(x)]$  is injective, so  $\text{MMD}(P, Q) = 0$  if and only if  $P = Q$ , and the MMD is a distance metric. For sample sets  $\mathcal{D} = \{x_i\}_{i=1}^m \sim P^m$ ,  $\tilde{\mathcal{D}} = \{\tilde{x}_i\}_{i=1}^n \sim Q^n$ , we also write

$$\text{MMD}(\mathcal{D}, \tilde{\mathcal{D}}) = \left\| \frac{1}{m} \sum_{i=1}^m \phi(\mathbf{x}_i) - \frac{1}{n} \sum_{i=1}^n \phi(\tilde{\mathbf{x}}_i) \right\|, \quad (1)$$

which is the “plug-in” estimator for  $\text{MMD}(P, Q)$  based on the empirical distributions of the datasets.

For differentially private data generation, we assume  $P$  is a data distribution and  $Q$  is a synthetic data distribution, the outputs of a generator. If the feature map is finite-dimensional and norm-bounded, like those in [6, 15], we can privatize the mean embedding of the data distribution  $\mathbb{E}_{x \sim P}[\phi(x)]$  with a known DP mechanism such as the Gaussian or Laplace mechanisms, discussed shortly. As the summary of the real data does not change over the course of a generator training, we need the privatization step only once, and continue using it repeatedly during the generator training.

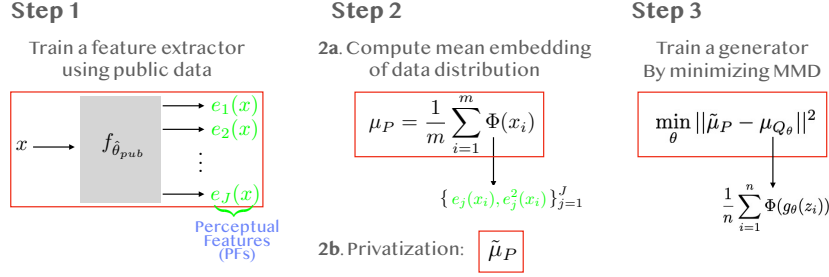


Figure 1: Three steps in *differentially private mean embedding with perceptual features (DP-MEPF)*. **Step 1:** We train a feature extractor neural network using public data. We denote the trained feature extractor by  $f_{\hat{\theta}_{pub}}$  to emphasize that this is a function of public data, and hence we do not pay the privacy budget on training the feature extractor. Once trained,  $f_{\hat{\theta}_{pub}}$  maps an input  $\mathbf{x}$  to perceptual features (in green), the outputs of each layer. **Step 2:** We compute the mean embedding of the data distributions using a feature map that consists of the first and second moments (in green) of the perceptual features. **Step 3:** We then privatize the mean embedding of the data distribution by the Gaussian mechanism (see text). Using the privatized mean embedding  $\tilde{\mu}_P$ , we train a generator  $g_{\theta}$  by minimizing the corresponding MMD, where  $g$  maps a sample  $z_i \sim \mathcal{N}(0, I)$  to a synthetic datapoint.

**Differential privacy** A mechanism  $\mathcal{M}$  is  $(\epsilon, \delta)$ -DP for a given  $\epsilon \geq 0$  and  $\delta \geq 0$  if and only if  $\Pr[\mathcal{M}(\mathcal{D}) \in S] \leq e^{\epsilon} \cdot \Pr[\mathcal{M}(\mathcal{D}') \in S] + \delta$  for all possible sets of the mechanism’s outputs  $S$  and all neighbouring datasets  $\mathcal{D}, \mathcal{D}'$  that differ by a single entry. One of the most well-known and widely used DP mechanisms is *Gaussian mechanism*. Consider a function  $\mu : \mathcal{D} \mapsto \mathbb{R}^p$ . The Gaussian mechanism adds a calibrated level of noise to the function to ensure that the output of the mechanism is  $(\epsilon, \delta)$ -DP:  $\tilde{\mu}(\mathcal{D}) = \mu(\mathcal{D}) + n$ , where  $n \sim \mathcal{N}(0, \sigma^2 \Delta_{\mu}^2 \mathbf{I}_p)$ . Here,  $\sigma$  is often called a privacy parameter, which is a function<sup>1</sup> of  $\epsilon$  and  $\delta$ .  $\Delta_{\mu}$  is often called the *global sensitivity* [10], which is the maximum difference in  $L_2$ -norm given two neighbouring  $\mathcal{D}$  and  $\mathcal{D}'$ ,  $\|\mu(\mathcal{D}) - \mu(\mathcal{D}')\|_2$ . In this paper, we will use the Gaussian mechanism to ensure the mean embedding of the data distribution is DP.

### 3 Method

In this paper, to transfer knowledge from public to private data distributions, we construct a particular kernel  $k_{\Phi}$  (to be used in MMD shown in eq. 1) using *Perceptual features* (PFs).

#### 3.1 MMD with perceptual features as a feature map

We call our proposed method *differentially private mean embeddings with perceptual features (DP-MEPF)* (analogously to the related method DP-MERF [15]). We use high-dimensional, over-complete perceptual features from a feature extractor network pre-trained on a public dataset, as illustrated in **Step 1** of Fig. 1. Given a vector input  $\mathbf{x}$ , the pre-trained feature extractor network outputs the perceptual features from each layer, where the  $j$ th layer’s PF is denoted by  $\mathbf{e}_j(\mathbf{x})$ . Each layer’s perceptual feature is of a different length,  $\mathbf{e}_j(\mathbf{x}) \in \mathbb{R}^{d_j}$  for  $j = 1, \dots, J$ , and the total dimension of the perceptual feature vector is denoted by  $D = \sum_{j=1}^J d_j$ .

As illustrated in **Step 2** in Fig. 1, we use those PFs to form our feature map  $\Phi(\mathbf{x}) := [\phi_1(\mathbf{x}), \phi_2(\mathbf{x})]$ , where the first part comes from a concatenation of PFs from all the layers:  $\phi_1(\mathbf{x}) = [\mathbf{e}_1(\mathbf{x}), \mathbf{e}_2(\mathbf{x}), \dots, \mathbf{e}_J(\mathbf{x})]$ , while the second part comes from their squared values:  $\phi_2(\mathbf{x}) = [\mathbf{e}_1^2(\mathbf{x}), \mathbf{e}_2^2(\mathbf{x}), \dots, \mathbf{e}_J^2(\mathbf{x})]$ , where  $\mathbf{e}_j^2(\mathbf{x})$  means each entry of  $\mathbf{e}_j(\mathbf{x})$  is squared. Using this feature map, we then construct the mean embedding of a data distribution given the data samples  $\mathcal{D} = \{\mathbf{x}_i\}_{i=1}^m$ :

$$\mu_P(\mathcal{D}) = \begin{bmatrix} \mu_P^{\phi_1}(\mathcal{D}) \\ \mu_P^{\phi_2}(\mathcal{D}) \end{bmatrix} = \begin{bmatrix} \frac{1}{m} \sum_{i=1}^m \phi_1(\mathbf{x}_i) \\ \frac{1}{m} \sum_{i=1}^m \phi_2(\mathbf{x}_i) \end{bmatrix} \quad (2)$$

<sup>1</sup>The relationship can be numerically computed by packages like `auto-dp` [44], among other methods.

As illustrated in **Step 3** in Fig. 1, we consider a generator  $g_\theta$  that maps a sample from a known distribution  $\mathbf{z}_i \sim \mathcal{N}(0, I)$  to a synthetic data sample  $\tilde{\mathbf{x}}_i = g_\theta(\mathbf{z}_i)$ , where  $\theta$  is the parameters of the generator  $g$  which we need to estimate. In non-private settings, we estimate the generator’s parameters by minimizing

$$\text{MMD}_{k_\Phi}^2(\mathcal{D}, \tilde{\mathcal{D}}) = \|\mu_P(\mathcal{D}) - \mu_{Q_{g_\theta}}(\tilde{\mathcal{D}})\|^2 \approx \text{MMD}_{k_\Phi}^2(P, Q_{g_\theta}) \quad (3)$$

where the mean embedding of the synthetic data distribution is given by  $\mu_{Q_{g_\theta}}(\tilde{\mathcal{D}}) = \frac{1}{n} \sum_{i=1}^n \Phi(\tilde{\mathbf{x}}_i)$  given a synthetic dataset  $\tilde{\mathcal{D}} = \{\tilde{\mathbf{x}}_i\}_{i=1}^n$ . In private settings, we privatize the mean embedding of the data distribution using the Gaussian mechanism, denoted by  $\tilde{\mu}_P$  (details below), and minimize

$$\widetilde{\text{MMD}}_{k_\Phi}^2(\mathcal{D}, \tilde{\mathcal{D}}) = \|\tilde{\mu}_P(\mathcal{D}) - \mu_{Q_{g_\theta}}(\tilde{\mathcal{D}})\|^2 \approx \widetilde{\text{MMD}}_{k_\Phi}^2(P, Q_{g_\theta}). \quad (4)$$

Extending our framework to generate both labels and input images is straightforward. As done in [15], we construct each mean embedding of input data per class and concatenate them, such that the size of the final mean embedding is  $D$  (number of perceptual features) by the number of classes if we use only the first moment, or  $2D$  by the number of classes if we use both moments.

A natural question that arises is whether the MMD using the PFs is a metric: if  $\text{MMD}_{k_\Phi}(P, Q) = 0$  only if  $P = Q$ . As PFs have a finite-dimensional embedding, we in fact know this cannot be the case [40]. Thus, there exists *some* pair of distributions which our MMD cannot distinguish. However, given that linear functions in perceptual feature spaces can obtain excellent performance on nearly any natural image task (as observed in transfer learning), it seems that PFs are “nearly” universal for natural distributions of images [9]. Thus we expect the MMD with this kernel to do a good job of distinguishing “natural” distributions from one another, though the possibility of distributions of “adversarial attacks” perhaps remains.

Regardless, a more useful and important question in our context is whether this MMD serves as a good loss for training a generator, and whether the resulting synthetic data samples are reasonably faithful to the original data samples. Our experiments in Sec. 6, as well as earlier work by dos Santos et al. [9] in non-private settings, imply that it is.

**Privatization of mean embedding** We privatize the mean embedding of the data distribution only once, and reuse it repeatedly during the training of the generator  $g_\theta$ . We use the Gaussian mechanism to separately privatize the first and second parts of the feature map. Typically,  $\phi_1$  and  $\phi_2$  are not norm-bounded, while using some form of normalization in each layer can induce the norm-boundedness in the resulting features. For the features that are not norm bounded, we clip the norm of these features such that  $\|\phi_1(\mathbf{x}_i)\| \leq C_1$  and  $\|\phi_2(\mathbf{x}_i)\| \leq C_2$  for all  $i = 1, \dots, m$ . After clipping, the sensitivity of each part of the mean embedding becomes simply

$$\max_{\mathcal{D}, \mathcal{D}' \text{ s.t. } |\mathcal{D} - \mathcal{D}'| = 1} \|\mu_P^{\phi_t}(\mathcal{D}) - \mu_P^{\phi_t}(\mathcal{D}')\|_2 \leq \frac{2C_t}{m}, \quad (5)$$

where each part of mean embedding is denoted by  $\mu_P^{\phi_t}(\mathcal{D})$  for  $t = 1, 2$ . Using these sensitivities, we add Gaussian noise to each part of the mean embedding, obtaining

$$\tilde{\mu}_P(\mathcal{D}) = \begin{bmatrix} \tilde{\mu}_P^{\phi_1}(\mathcal{D}) \\ \tilde{\mu}_P^{\phi_2}(\mathcal{D}) \end{bmatrix} = \begin{bmatrix} \frac{1}{m} \sum_{i=1}^m \phi_1(\mathbf{x}_i) + \eta_1 \\ \frac{1}{m} \sum_{i=1}^m \phi_2(\mathbf{x}_i) + \eta_2 \end{bmatrix}, \quad (6)$$

where  $\eta_t \sim \mathcal{N}(0, \sigma^2(\frac{2C_t}{m})^2 I)$  for  $t = 1, 2$ .

Since we are using the Gaussian mechanism twice, we simply compose the privacy losses from each mechanism. More precisely, given a desired privacy level  $\epsilon, \delta$ , we use the package of Wang et al. [44] to find the corresponding  $\sigma$  for the two Gaussian mechanisms.

## 4 Theoretical analysis of DP-MEPF

We first focus on quantifying the effect of noise on the loss function itself; we will turn to the resulting error in the loss afterwards. We start by bounding the mean absolute error between the privatized MMD and non-private MMD, given samples from  $P, Q$ . For notational simplicity, here we assume we use only the first moment of the PFs for the mean embeddings, i.e.,  $\mu_P = \mu_P^{\phi_1}$  and  $\mu_Q = \mu_Q^{\phi_1}$ , and that also we have one clipping bound  $C = C_1$  as a result. Extending the result to the case using both first and second moments of the PFs is straightforward; see Appendix Sec. B.

**Proposition 4.1.** *Given datasets  $\mathcal{D} = \{\mathbf{x}_i\}_{i=1}^m$  and  $\tilde{\mathcal{D}} = \{\tilde{\mathbf{x}}_j\}_{j=1}^n$ , the expected absolute error between the privatized MMD and the non-private MMD is bounded by*

$$\mathbb{E}_{\mathbf{n}} \left[ \left| \widetilde{\text{MMD}}_{k_{\Phi}}^2(\mathcal{D}, \tilde{\mathcal{D}}) - \text{MMD}_{k_{\Phi}}^2(\mathcal{D}, \tilde{\mathcal{D}}) \right| \right] \leq \frac{4\sigma^2 C^2}{m^2} D + \frac{4\sigma C}{m} \sqrt{\frac{2}{\pi}} \text{MMD}_{k_{\Phi}}(\mathcal{D}, \tilde{\mathcal{D}}). \quad (7)$$

The proof, in Appendix Sec. A, simply rearranges eq. 3 and 4 and then bounds the added noise.

This bound depends on three quantities. One key quantity is  $\sigma C/m$ , the product of the noise scale  $\sigma$  (inversely proportional to  $\varepsilon$ ), and the clipping norm  $C$  divided by the number of observed (private) data points  $m$ . Note that  $\sigma$  depends only on the given privacy level, not on  $m$ , so the error becomes zero as long as  $C/m \rightarrow 0$ ; though this allows  $C$  to grow with  $m$ , in practice we use  $C = 1$ .

In the second term of the bound,  $\sigma C/m$  is multiplied by the (non-private, non-squared) MMD, which is always bounded by  $2C$ , but for good generators (where our optimization hopefully spends most of its time) this term will also be nearly zero. The other term accounts for adding independent noise to each of the  $D$  feature dimensions; although  $D$  is typically large, so is  $m^2$ . Having  $m = 50\text{k}$  private samples, e.g. for CIFAR-10, allows for a strong expected error bound as long as  $D\sigma^2 C^2 \ll 625\text{M}$ .

Prop. 4.1 shows that the expected absolute error is low. We now use this to show a stronger, but slightly more complex, result: the absolute error is almost always small.

**Proposition 4.2.** *Let the non-private MMD between datasets  $\mathcal{D} = \{\mathbf{x}_i\}_{i=1}^m$  and  $\tilde{\mathcal{D}} = \{\tilde{\mathbf{x}}_j\}_{j=1}^n$  be  $M = \text{MMD}_{k_{\Phi}}(\mathcal{D}, \tilde{\mathcal{D}})$ . For any  $\rho > 0$ , the error  $|\widetilde{\text{MMD}}_{k_{\Phi}}^2(\mathcal{D}, \tilde{\mathcal{D}}) - \text{MMD}_{k_{\Phi}}^2(\mathcal{D}, \tilde{\mathcal{D}})|$  is at most*

$$\frac{4\sigma C}{m} \left[ \frac{\sigma C}{m} D + \sqrt{\frac{2}{\pi}} M + \left( \frac{2\sigma C}{m} \sqrt{D} + \frac{1}{\sqrt{2}} M \right) \sqrt{\log \frac{2}{\rho}} + \frac{2\sigma C}{m} \log \frac{2}{\rho} \right] \quad (8)$$

with probability at least  $1 - \rho$  over the choice of noise vector.

The proof, in Appendix Sec. C, relies on standard concentration inequalities for Lipschitz functions of Gaussian random variables. Notice that the first two terms are exactly the bound on the expected absolute error in Prop. 4.1. The other two terms establish a mixture of a sub-Gaussian tail (the  $\sqrt{\log \frac{2}{\rho}}$  term) with a (heavier) sub-exponential tail (the  $\log \frac{2}{\rho}$  term), whose weights also go to zero with essentially the same trade-offs as the expected error.

Notice that eq. 8 depends on the generator only via  $\text{MMD}_{k_{\Phi}}(\mathcal{D}, \tilde{\mathcal{D}})$ ; the randomness is entirely due to the Gaussian noise vector, which we add to  $\mu_P(\mathcal{D})$  *only once*. Thus, plugging in the worst-case bound  $\text{MMD}_{k_{\Phi}}(\mathcal{D}, \tilde{\mathcal{D}}) \leq 2C$  to eq. 8, we immediately obtain a *uniform convergence* bound:

**Proposition 4.3.** *Fix  $\mathcal{D} = \{\mathbf{x}_i\}_{i=1}^m$ . Then, for any  $\rho > 0$ , we have with probability at least  $1 - \rho$  over the choice of noise vector that*

$$\sup_{n \geq 0, \tilde{\mathcal{D}} \in \mathcal{X}^n} |\widetilde{\text{MMD}}_{k_{\Phi}}^2(\mathcal{D}, \tilde{\mathcal{D}}) - \text{MMD}_{k_{\Phi}}^2(\mathcal{D}, \tilde{\mathcal{D}})| \leq \alpha$$

$$\text{where } \alpha := \frac{4\sigma C^2}{m} \left[ \frac{\sigma}{m} D + 2\sqrt{\frac{2}{\pi}} + 2 \left( \frac{\sigma}{m} \sqrt{D} + \frac{1}{\sqrt{2}} \right) \sqrt{\log \frac{2}{\rho}} + \frac{2\sigma}{m} \log \frac{2}{\rho} \right].$$

The immediacy of this proof is a benefit of applying the same noise vector everywhere; typically, these proofs require substantially more machinery. This bound is also extremely flexible, applying to *any* possible set  $\tilde{\mathcal{D}}$ , but has worsened our “optimistic”  $\mathcal{O}(\frac{1}{m^2} + \frac{M}{m})$  rate to  $\mathcal{O}(\frac{1}{m})$ .

Now, finally, we have that minimizing the private MMD approximately minimizes non-private MMD.

**Proposition 4.4.** *Fix a dataset  $\mathcal{D} = \{\mathbf{x}_i\}_{i=1}^m$ . For each  $\theta$  in some set  $\Theta$ , fix a corresponding  $\tilde{\mathcal{D}}_{\theta}$ ; in particular,  $\Theta = \mathbb{R}^p$  could be the set of all generator parameters, and  $\tilde{\mathcal{D}}_{\theta}$  the outcome of running a generator  $g_{\theta}$  on a fixed set of “seeds,”  $\tilde{\mathcal{D}}_{\theta} = \{g_{\theta}(\mathbf{z}_i)\}_{i=1}^n$ . Let  $\tilde{\theta} \in \arg \min_{\theta \in \Theta} \widetilde{\text{MMD}}_{k_{\Phi}}^2(\mathcal{D}, \tilde{\mathcal{D}}_{\theta})$  be the private minimizer, and  $\hat{\theta} \in \arg \min_{\theta \in \Theta} \text{MMD}_{k_{\Phi}}^2(\mathcal{D}, \tilde{\mathcal{D}}_{\theta})$  the non-private minimizer. For any  $\rho > 0$ , let  $\alpha$  be as in Prop. 4.3. Then, with probability at least  $1 - \rho$  over the choice of noise,*

$$\text{MMD}_{k_{\Phi}}^2(\mathcal{D}, \tilde{\mathcal{D}}_{\tilde{\theta}}) \leq \text{MMD}_{k_{\Phi}}^2(\mathcal{D}, \tilde{\mathcal{D}}_{\hat{\theta}}) + 2\alpha.$$

*Proof.* We use uniform convergence, the definition of  $\tilde{\theta}$ , then uniform convergence again:

$$\text{MMD}_{k_{\Phi}}^2(\mathcal{D}, \tilde{\mathcal{D}}_{\tilde{\theta}}) \leq \widetilde{\text{MMD}}_{k_{\Phi}}^2(\mathcal{D}, \tilde{\mathcal{D}}_{\tilde{\theta}}) + \alpha \leq \widetilde{\text{MMD}}_{k_{\Phi}}^2(\mathcal{D}, \tilde{\mathcal{D}}_{\theta}) + \alpha \leq \text{MMD}_{k_{\Phi}}^2(\mathcal{D}, \tilde{\mathcal{D}}_{\theta}) + 2\alpha. \quad \square$$

Thus, for any fixed private training dataset of size  $m$ , with any constant probability, we have that private training introduces suboptimality (measured by the MMD) of at most  $\mathcal{O}\left(\frac{\sigma C^2}{m} \left[1 + \frac{\sigma D}{m}\right]\right)$ .

This result says that we nearly minimize the non-private MMD estimate. Then, based on uniform convergence of the plug-in MMD estimator to its population value, this implies that  $\tilde{\theta}$  will also nearly minimize  $\text{MMD}_{k_{\Phi}}(P, Q_{g_{\theta}})$ ; see Theorem 1 of Briol et al. [4] or of Dziugaite et al. [11].

## 5 Related Work

Initial works on differentially private data generation assume strong constraints on the type of data and the intended use of the released data [17, 28, 39, 47, 53]. While these works provide theoretical guarantees on the utility of the synthetic data, they typically do not scale to large-scale image data generation, which is our goal.

Recently, several works focus on discrete data generation with limited domain size [8, 34, 50, 51]. These methods learn the correlation structure of small subsets of features and privatize them in order to produce differentially private synthetic data samples. These methods often require discretization of the data and have limited scalability, which makes these methods not suitable for high-dimensional image data generation.

More recently, however, a new line of work has emerged that adopt the core ideas from the recent advances in deep generative models for a broad applicability of synthetic data with differential private constraints. The majority of work in this line of research uses the generative adversarial networks (GANs) [7, 12, 42, 48, 49], which uses some forms of DP-SGD [1]. Other works in this line include PATE-GAN based on the private aggregation of teacher ensembles (PATE) [30] and VAEs [2].

The closest prior work to the proposed method is DP-MERF [15], where the kernel mean embeddings are constructed using random Fourier features [35]. A recent variant of DP-MERF uses a Hermite-Polynomial-based mean embeddings [6]. Unlike these methods, we use the perceptual features from a pre-trained network to construct kernel mean embeddings. Neither previous method applies to the perceptual kernels used here, so their empirical results are far worse (as we’ll see shortly), and our theoretical analysis is also far more extensive: they proved only an analogue of our Prop. 4.1.

More recently, a similar work to DP-MERF utilizes the Sinkhorn divergence for private data generation [5], which performs similarly to DP-MERF when the cost function is the L2 distance with a large regularizer. Another related work proposes to use the characteristic function and an adversarial re-weighting objective [25] in order to improve the generalization capability of DP-MERF.

The performance of all of the aforementioned methods, however, was evaluated on generating relatively simple datasets such as MNIST and FashionMNIST. Even for these simple datasets, most of the DP-GAN-based methods require a large privacy budget of  $\epsilon \approx 10$  to generate synthetic data samples that are close enough to the real data samples. Our method goes far beyond what these methods can produce with much more stringent privacy constraints, as illustrated in Sec. 6.

## 6 Experiments

Here, we demonstrate the performance of our method in comparison with the state-of-the-art methods in DP data generation.

*Datasets.* We considered four image datasets<sup>2</sup> of varying complexity. We started with the commonly used datasets MNIST [23] and FashionMNIST [45], where each consist of 60,000 28x28 pixel grayscale images depicting hand-written digits and items of clothing, respectively, sorted into 10 classes. With an increasing complexity, we also looked at CelebA [26], a dataset containing 202,599 color images of faces which we scale to a size of 32x32 pixels. We used CelebA as an unlabeled

<sup>2</sup>Dataset licenses: MNIST: CC BY-SA 3.0; FashionMNIST:MIT; CelebA: see <https://mmlab.ie.cuhk.edu.hk/projects/CelebA.html>; Cifar10: MIT

Table 1: Downstream accuracies by Logistic regression and MLP, evaluated on the generated data samples using MNIST and FashionMNIST as private data and SVHN and CIFAR-10 as public data, respectively. In all cases, we set  $\epsilon = 10$ ,  $\delta = 1e^{-5}$ . In our method, we used both features  $\phi_1, \phi_2$ .

		DP-MEPF	DP-Sinkhorn [5]	GS-WGAN [7]	DP-MERF [15]	DP-HP [6]
MNIST	LogReg	<b>83</b>	83	79	79	81
	MLP	<b>90</b>	83	79	78	82
F-MNIST	LogReg	<b>76</b>	75	68	76	73
	MLP	<b>76</b>	75	65	75	71

Table 2: Downstream accuracies of our method for MNIST and FashionMNIST at varying values of  $\epsilon$

		MNIST				FashionMNIST			
		$\epsilon = 5$	$\epsilon = 2$	$\epsilon = 1$	$\epsilon = 0.2$	$\epsilon = 5$	$\epsilon = 2$	$\epsilon = 1$	$\epsilon = 0.2$
MLP	DP-MEPF ( $\phi_1, \phi_2$ )	90	89	89	80	76	75	75	70
	DP-MEPF ( $\phi_1$ )	88	88	87	77	75	76	75	69
LogReg	DP-MEPF ( $\phi_1, \phi_2$ )	83	83	82	76	75	76	75	73
	DP-MEPF ( $\phi_1$ )	81	80	79	72	75	76	76	72

dataset. Lastly, we present results on CIFAR-10 [20], a 50,000-sample dataset containing 32x32-dimensional color images depicting 10 classes of objects including vehicles like ships and trucks and animals such as horses and birds.

*Implementation.* We implemented our code for all the experiments in PyTorch [32], using the auto-dp package<sup>3</sup> for the privacy analysis. Following [15], we used the generator that consists of two fully connected layers followed by two convolutional layers with bilinear upsampling, for generating both MNIST and FashionMNIST datasets. For MNIST, we used the SVHN dataset as public data to pre-train ResNet18 [18], from which we took the perceptual features. For FashionMNIST, we used the CIFAR-10 dataset as public data and trained ResNet18 whose features we used as perceptual features. For CelebA and CIFAR-10 datasets, we took the pre-trained VGG [37] using ImageNet data from [9] and used its perceptual features. Following [9], we used ResNet18 as a generator for these two datasets. Due to the space limit, the rest of the implementation details are given in the Appendix.

*Evaluation metric.* Evaluating the quality of generated data is challenging on its own. Hence, we follow the convention in the literature and use the two measures. The first one is the *Frechet Inception Distance (FID)* score [19], which directly measures the quality of the generated samples. The FID score is considered a good approximation of visual similarity with the real data as experienced by humans, and hence commonly used in deep generative modelling. We computed FID scores with the `pytorch_fid` package [36], based on 5000 generated samples, matching [9]. The second one is the accuracy of downstream classifiers, which we train using the generated datasets and then test on the real data test sets, as used in [5, 7, 15, 42, 49]. This test accuracy indicates how well the downstream classifiers generalize from the synthetic to the real data distribution and thus, the utility of using synthetic data samples instead of the real ones. We computed the downstream accuracy on MNIST and FashionMNIST using the logistic regression and MLP classifiers from `scikit-learn` [33]. For CIFAR-10, we used ResNet9 taken from FFCV<sup>4</sup> [22].

In all experiments, we tested a non-DP training and then private settings with a varying level of privacy, ranging from  $\epsilon = 10$  (no meaningful guarantee) to  $\epsilon = 0.2$  (strong privacy guarantee). In all cases, we set  $\delta = 10^{-5}$ . In DP-MEPF, we also tested two cases where we match mean embeddings using only the first moment (we put  $\phi_1$  to indicate this) and using both moments (we put  $\phi_1$  and  $\phi_2$  to indicate this). Note that each value in all tables is an average across 3 independent runs. Results including standard deviation are found in the Appendix.

Since no prior work has published results on DP data generation for image data using auxiliary datasets, we instead compare to recent methods which do not access auxiliary data. As expected, due to the advantage of non-private data our approach outperforms these methods by a significant margin on the more complex datasets.

<sup>3</sup><https://github.com/yuxiangw/autodp>

<sup>4</sup>[https://github.com/libffcv/ffcv/blob/main/examples/cifar/train\\_cifar.py](https://github.com/libffcv/ffcv/blob/main/examples/cifar/train_cifar.py)

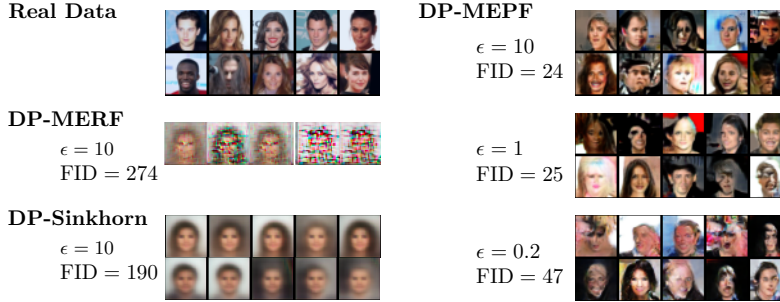


Figure 2: Synthetic CelebA samples generated at different levels of privacy along with their FID score. Samples for DP-MERF and DP-Sinkhorn are taken from [5]. Even at  $\epsilon = 0.2$ , DP-MEPF ( $\phi_1, \phi_2$ ) outperforms the comparison methods which do not use auxiliary data.

Table 3: CelebA FID scores (lower is better)

	$\epsilon = \infty$	$\epsilon = 10$	$\epsilon = 5$	$\epsilon = 2$	$\epsilon = 1$	$\epsilon = 0.2$
DP-MEPF ( $\phi_1, \phi_2$ )	24.53	25.84	24.14	25.51	23.28	42.44
DP-MEPF ( $\phi_1$ )	23.35	23.77	22.79	26.02	25.41	46.55

**MNIST and FashionMNIST.** As they are currently the most common image datasets used in the literature, we compare DP-MEPF to existing methods on MNIST and FashionMNIST. In table 1, the MLP trained with generated samples by DP-MEPF outperforms existing methods by a large margin in case of MNIST. In case of FashionMNIST, the scores for DP-MEPF match or slightly exceed those of existing models. This might be because the domain shift between public (CIFAR-10, coloured images) and private (FashionMNIST, greyscale images) dataset is too large or because the task is simple enough that random features as found in DP-MERF or DP-HP are already good enough. This will change as we proceed to more complex datasets.

In 2 we see that downstream test accuracy only starts to drop in the high privacy regime at  $\epsilon < 1$ . This robustness is owed to the low sensitivity of the released embedding. Samples for visual comparison between methods are included in the Appendix.

**CelebA** In Fig. 2, one can see that previous attempts to generate CelebA samples without auxiliary data using DP-MERF or DP-Sinkhorn have only managed to capture very basic features of the data. The images show that each sample depicts a face but offer no details or variety. DP-MEPF produces more accurate samples, which is also reflected in improved FID scores of around 25 compared to 190 for DP-Sinkhorn, shown next to the samples. Thanks to the large dataset with over 200.000 samples, the feature embeddings have low sensitivity and offer similar quality between  $\epsilon = 10$  and  $\epsilon = 1$ . At  $\epsilon = 0.2$ , we observe a significant increase in FID along with a visible drop in sample quality. Table 3 shows FID scores of our method at varying  $\epsilon$ .

**CIFAR-10** Finally, we investigate a dataset which has not been covered in DP data generation, due to its complexity. While CelebA depicts a centered face in every image, CIFAR-10 includes 10 visually distinct object classes, which raises the required minimum quality of samples to somewhat resemble the dataset. At only 5,000 samples per class, the dataset is also significantly smaller, which poses a challenge in the private setting.

Fig. 3 shows that DP-MEPF is capable of producing labelled private data (generating both labels and input images together) resembling the real data, but the quality does suffer severely compared to the non-private setting. This is also reflected in the associated FID scores shown in Table 4 (left-hand side) where non-DP MEPF achieves a score of 45 while the private version, even at  $\epsilon = 10$  only gets a score of 85.

Interestingly, the effect of privacy on downstream classification is less significant than the increase in FID. Table 5 shows that the test



Figure 4: Unlabelled CIFAR-10 samples from DP-MEPF ( $\phi_1, \phi_2$ ). Compared to Fig. 3, image quality degrades less in high privacy settings.



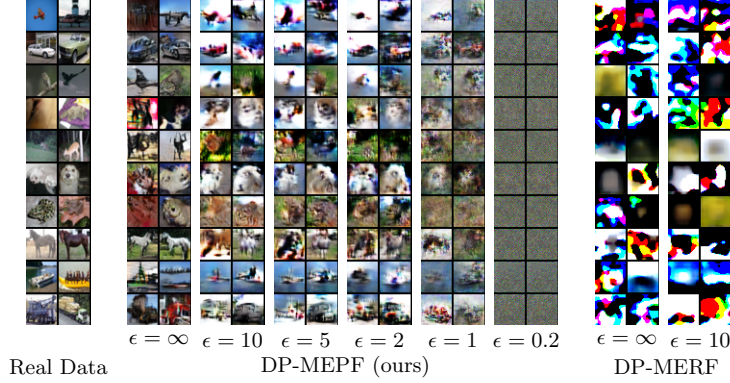


Figure 3: Labelled CIFAR-10 samples from DP-MEPF ( $\phi_1, \phi_2$ ) and DP-MERF [15] at different levels of privacy.

Table 4: FID scores for synthetic CIFAR-10 data; labeled generates both labels and images.

	labeled						unlabeled			
	$\epsilon = \infty$	$\epsilon = 10$	$\epsilon = 5$	$\epsilon = 2$	$\epsilon = 1$	$\epsilon = 0.2$	$\epsilon = \infty$	$\epsilon = 5$	$\epsilon = 2$	$\epsilon = 1$
<b>DP-MEPF</b> ( $\phi_1, \phi_2$ )	45	85	83	92	103	367	45	51	54	64
<b>DP-MEPF</b> ( $\phi_1$ )	45	90	91	95	114	491	39	49	52	64
DP-MERF	127	124	124	126	123	413				

accuracy on real data hardly changes when depending on whether generated samples are trained on non-private or ( $\epsilon = 10, \delta = 10^{-5}$ )-DP synthetic data. Accuracy does of course go down for higher levels of privacy and is at chance level for  $\epsilon = 0.2$ . Along with our approach we present results for DP-MERF to illustrate that its random features are insufficient for modeling data of this complexity. FID scores are high and accuracy is barely above a chance level for all levels of privacy.

While the drop in sample quality due to privacy is quite substantial in the private setting, we can show that is less of a problem in the unlabeled case, since our embedding is smaller by a factor of 10 (i.e. the number of classes) and thus easier to release privately. The FID scores in Table 4 (right hand side) and corresponding samples in Fig. 4 show that unlabeled sample quality at  $\epsilon = 1$  remains higher than that of labeled samples  $\epsilon = 10$ .

Table 5: Test accuracies (higher better) of ResNet9 trained on CIFAR-10 synthetic data with varying privacy guarantees. When trained on real data, test accuracy is 88.3%

	$\epsilon = \infty$	$\epsilon = 10$	$\epsilon = 5$	$\epsilon = 2$	$\epsilon = 1$	$\epsilon = 0.2$
<b>DP-MEPF</b> ( $\phi_1$ )	54.9	52.4	49.9	47.6	32.8	10.2
<b>DP-MEPF</b> ( $\phi_1, \phi_2$ )	54.0	54.4	50.1	45.8	34.9	11.8
DP-MERF	13.2	13.4	13.5	13.8	13.1	10.4

## 7 Conclusion and Future Directions

We have demonstrated the advantage of using auxiliary public data in DP data generation. Our method DP-MEPF takes advantage of features from pre-trained classifiers that are readily available and allows us to tackle datasets like CelebA and CIFAR-10, which have been unreachable for private data generation up to this point.

There are several avenues to extend our method in future work, starting with a closer look at the selection of the encoder. VGG19 was chosen in [9] and works well in the private settings. However, since the private setting favours smaller embeddings, which are more robust to noise, the choice is likely not optimal. Pruning uninformative and redundant features from a classifier also promises to improve the utility privacy trade-off.

Training other generative models such as GANs or VAEs with pretrained components is also a space worth exploring, however this will require multiple DP releases, likely at each iteration, in which case these models have a trouble achieving good results at  $\epsilon \leq 2$ . We believe that our method is more promising than those kinds of models because the single private release allows for strong privacy guarantees. The over-complete perceptual features also help overcome the major weakness of its predecessor DP-MERF, whose features were not able to generate diverse synthetic data samples.

## References

- [1] Martin Abadi, Andy Chu, Ian Goodfellow, H. Brendan McMahan, Ilya Mironov, Kunal Talwar, and Li Zhang. “Deep Learning with Differential Privacy.” *Proceedings of the 2016 ACM SIGSAC Conference on Computer and Communications Security*. CCS ’16. New York, NY, USA: Association for Computing Machinery, 2016, pp. 308–318.
- [2] Gergely Acs, Luca Melis, Claude Castelluccia, and Emiliano De Cristofaro. “Differentially private mixture of generative neural networks.” *IEEE Transactions on Knowledge and Data Engineering* 31.6 (2018), pp. 1109–1121.
- [3] S. Boucheron, G. Lugosi, and P. Massart. *Concentration inequalities: A nonasymptotic theory of independence*. Oxford University Press, 2013.
- [4] François-Xavier Briol, Alessandro Barp, Andrew B. Duncan, and Mark A. Girolami. *Statistical Inference for Generative Models with Maximum Mean Discrepancy*. 2019. arXiv: 1906.05944.
- [5] Tianshi Cao, Alex Bie, Arash Vahdat, Sanja Fidler, and Karsten Kreis. “Don’t Generate Me: Training Differentially Private Generative Models with Sinkhorn Divergence.” *Neural Information Processing Systems (NeurIPS)*. 2021.
- [6] Mohammad-Amin Charusaie, Margarita Vinaroz, Frederik Harder, Kamil Adamczewski, and Mijung Park. “Hermite polynomials for private data generation.” *CoRR* abs/2106.05042 (2021). arXiv: 2106.05042.
- [7] Dingfan Chen, Tribhuvanesh Orekondy, and Mario Fritz. “GS-WGAN: A Gradient-Sanitized Approach for Learning Differentially Private Generators.” *Advances in Neural Information Processing Systems* 33. 2020.
- [8] Rui Chen, Qian Xiao, Yu Zhang, and Jianliang Xu. “Differentially private high-dimensional data publication via sampling-based inference.” *Proceedings of the 21th ACM SIGKDD International Conference on Knowledge Discovery and Data Mining*. 2015, pp. 129–138.
- [9] Cícero Nogueira dos Santos, Youssef Mroueh, Inkit Padhi, and Pierre L. Dognin. “Learning Implicit Generative Models by Matching Perceptual Features.” *2019 IEEE/CVF International Conference on Computer Vision, ICCV 2019, Seoul, Korea (South), October 27 - November 2, 2019*. IEEE, 2019, pp. 4460–4469.
- [10] Cynthia Dwork, Krishnaram Kenthapadi, Frank McSherry, Ilya Mironov, and Moni Naor. “Our Data, Ourselves: Privacy Via Distributed Noise Generation.” *Eurocrypt*. Vol. 4004. Springer, 2006, pp. 486–503.
- [11] Gintare Karolina Dziugaite, Daniel M. Roy, and Zoubin Ghahramani. “Training generative neural networks via Maximum Mean Discrepancy optimization.” *UAI*. 2015. arXiv: 1505.03906.
- [12] Lorenzo Frigerio, Anderson Santana de Oliveira, Laurent Gomez, and Patrick Duverger. “Differentially Private Generative Adversarial Networks for Time Series, Continuous, and Discrete Open Data.” *ICT Systems Security and Privacy Protection - 34th IFIP TC 11 International Conference, SEC 2019, Lisbon, Portugal, June 25-27, 2019, Proceedings*. 2019, pp. 151–164.
- [13] Ian Goodfellow, Jean Pouget-Abadie, Mehdi Mirza, Bing Xu, David Warde-Farley, Sherjil Ozair, Aaron Courville, and Yoshua Bengio. “Generative Adversarial Nets.” *Advances in Neural Information Processing Systems* 27. Ed. by Z. Ghahramani, M. Welling, C. Cortes, N. D. Lawrence, and K. Q. Weinberger. Curran Associates, Inc., 2014, pp. 2672–2680.
- [14] Arthur Gretton, Karsten M Borgwardt, Malte J Rasch, Bernhard Schölkopf, and Alexander Smola. “A kernel two-sample test.” *Journal of Machine Learning Research* 13.Mar (2012), pp. 723–773.
- [15] Frederik Harder, Kamil Adamczewski, and Mijung Park. “DP-MERF: Differentially Private Mean Embeddings with Random Features for Practical Privacy-preserving Data Generation.” *Proceedings of The 24th International Conference on Artificial Intelligence and Statistics*. Ed. by Arindam Banerjee and Kenji Fukumizu. Vol. 130. Proceedings of Machine Learning Research. PMLR, 2021, pp. 1819–1827.
- [16] Moritz Hardt, Katrina Ligett, and Frank Mcsherry. “A Simple and Practical Algorithm for Differentially Private Data Release.” *Advances in Neural Information Processing Systems* 25. Ed. by F. Pereira, C. J. C. Burges, L. Bottou, and K. Q. Weinberger. Curran Associates, Inc., 2012, pp. 2339–2347.

- [17] Moritz Hardt, Katrina Ligett, and Frank Mcsherry. “A Simple and Practical Algorithm for Differentially Private Data Release.” *Advances in Neural Information Processing Systems* 25. Ed. by F. Pereira, C. J. C. Burges, L. Bottou, and K. Q. Weinberger. Curran Associates, Inc., 2012, pp. 2339–2347.
- [18] Kaiming He, Xiangyu Zhang, Shaoqing Ren, and Jian Sun. “Deep residual learning for image recognition.” *Proceedings of the IEEE conference on computer vision and pattern recognition*. 2016, pp. 770–778.
- [19] Martin Heusel, Hubert Ramsauer, Thomas Unterthiner, Bernhard Nessler, and Sepp Hochreiter. “Gans trained by a two time-scale update rule converge to a local nash equilibrium.” *Advances in neural information processing systems* 30 (2017).
- [20] Alex Krizhevsky, Geoffrey Hinton, et al. “Learning multiple layers of features from tiny images” (2009).
- [21] Beatrice Laurent and Pascal Massart. “Adaptive estimation of a quadratic functional by model selection.” *Annals of Statistics* (2000), pp. 1302–1338.
- [22] Guillaume Leclerc, Andrew Ilyas, Logan Engstrom, Sung Min Park, Hadi Salman, and Aleksander Madry. *ffcv*. <https://github.com/libffcv/ffcv/>. 2022.
- [23] Yann LeCun and Corinna Cortes. “MNIST handwritten digit database” (2010).
- [24] Yujia Li, Kevin Swersky, and Richard S. Zemel. “Generative Moment Matching Networks.” *ICML*. 2015. arXiv: 1502.02761.
- [25] Seng Pei Liew, Tsubasa Takahashi, and Michihiko Ueno. “PEARL: Data Synthesis via Private Embeddings and Adversarial Reconstruction Learning.” *International Conference on Learning Representations*. 2022.
- [26] Ziwei Liu, Ping Luo, Xiaogang Wang, and Xiaoou Tang. “Deep Learning Face Attributes in the Wild.” *Proceedings of International Conference on Computer Vision (ICCV)*. Dec. 2015.
- [27] Noman Mohammed, Rui Chen, Benjamin C.M. Fung, and Philip S. Yu. “Differentially Private Data Release for Data Mining.” *Proceedings of the 17th ACM SIGKDD International Conference on Knowledge Discovery and Data Mining*. KDD ’11. New York, NY, USA: ACM, 2011, pp. 493–501.
- [28] Noman Mohammed, Rui Chen, Benjamin C.M. Fung, and Philip S. Yu. “Differentially Private Data Release for Data Mining.” *Proceedings of the 17th ACM SIGKDD International Conference on Knowledge Discovery and Data Mining*. KDD ’11. New York, NY, USA: ACM, 2011, pp. 493–501.
- [29] National Conference of State Legislatures. *Differentially privacy for census data*. 2021.
- [30] Nicolas Papernot, Martín Abadi, Úlfar Erlingsson, Ian Goodfellow, and Kunal Talwar. “Semi-supervised Knowledge Transfer for Deep Learning from Private Training Data.” *Proceedings of the International Conference on Learning Representations (ICLR)*. Apr. 2017. arXiv: 1610.05755.
- [31] Mijung Park, James Foulds, Kamalika Choudhary, and Max Welling. “DP-EM: Differentially Private Expectation Maximization.” *Proceedings of the 20th International Conference on Artificial Intelligence and Statistics*. Ed. by Aarti Singh and Jerry Zhu. Vol. 54. Proceedings of Machine Learning Research. Fort Lauderdale, FL, USA: PMLR, Apr. 2017, pp. 896–904.
- [32] Adam Paszke et al. “PyTorch: An Imperative Style, High-Performance Deep Learning Library.” *Advances in Neural Information Processing Systems* 32. Ed. by H. Wallach, H. Larochelle, A. Beygelzimer, F. d’Alché-Buc, E. Fox, and R. Garnett. Curran Associates, Inc., 2019, pp. 8024–8035.
- [33] F. Pedregosa et al. “Scikit-learn: Machine Learning in Python.” *Journal of Machine Learning Research* 12 (2011), pp. 2825–2830.
- [34] Wahbeh Qardaji, Weining Yang, and Ninghui Li. “Priview: practical differentially private release of marginal contingency tables.” *Proceedings of the 2014 ACM SIGMOD international conference on Management of data*. 2014, pp. 1435–1446.
- [35] Ali Rahimi and Benjamin Recht. “Random features for large-scale kernel machines.” *Advances in neural information processing systems*. 2008, pp. 1177–1184.
- [36] Maximilian Seitzer. *pytorch-fid: FID Score for PyTorch*. <https://github.com/mseitzer/pytorch-fid>. Version 0.2.1. Aug. 2020.
- [37] Karen Simonyan and Andrew Zisserman. “Very deep convolutional networks for large-scale image recognition.” *arXiv preprint arXiv:1409.1556* (2014).

- [38] A. Smola, A. Gretton, L. Song, and B. Schölkopf. “A Hilbert space embedding for distributions.” *ALT*. 2007, pp. 13–31.
- [39] Joshua Snok and Aleksandra Slavković. “pMSE mechanism: differentially private synthetic data with maximal distributional similarity.” *International Conference on Privacy in Statistical Databases*. Springer. 2018, pp. 138–159.
- [40] Bharath K Sriperumbudur, Kenji Fukumizu, and Gert RG Lanckriet. “Universality, Characteristic Kernels and RKHS Embedding of Measures.” *Journal of Machine Learning Research* 12.7 (2011).
- [41] Differential Privacy Team. *Learning with Privacy at Scale*. 2017.
- [42] Reihaneh Torkzadehmahani, Peter Kairouz, and Benedict Paten. “DP-CGAN: Differentially Private Synthetic Data and Label Generation.” *The IEEE Conference on Computer Vision and Pattern Recognition (CVPR) Workshops*. June 2019.
- [43] Florian Tramer and Dan Boneh. “Differentially Private Learning Needs Better Features (or Much More Data).” *International Conference on Learning Representations*. 2021.
- [44] Yu-Xiang Wang, Borja Balle, and Shiva Prasad Kasiviswanathan. “Subsampled Rényi differential privacy and analytical moments accountant.” PMLR. 2019.
- [45] Han Xiao, Kashif Rasul, and Roland Vollgraf. “Fashion-MNIST: a Novel Image Dataset for Benchmarking Machine Learning Algorithms.” *ArXiv abs/1708.07747* (2017).
- [46] Yonghui Xiao, Li Xiong, and Chun Yuan. “Differentially Private Data Release through Multidimensional Partitioning.” *Secure Data Management*. Ed. by Willem Jonker and Milan Petković. Berlin, Heidelberg: Springer Berlin Heidelberg, 2010, pp. 150–168.
- [47] Yonghui Xiao, Li Xiong, and Chun Yuan. “Differentially Private Data Release through Multidimensional Partitioning.” *Secure Data Management*. Ed. by Willem Jonker and Milan Petković. Berlin, Heidelberg: Springer Berlin Heidelberg, 2010, pp. 150–168.
- [48] Liyang Xie, Kaixiang Lin, Shu Wang, Fei Wang, and Jiayu Zhou. “Differentially Private Generative Adversarial Network.” *CoRR abs/1802.06739* (2018). arXiv: 1802.06739.
- [49] Jinsung Yoon, James Jordon, and Mihaela van der Schaar. “PATE-GAN: Generating Synthetic Data with Differential Privacy Guarantees.” *International Conference on Learning Representations*. 2019.
- [50] Jun Zhang, Graham Cormode, Cecilia M Procopiuc, Divesh Srivastava, and Xiaokui Xiao. “Privbayes: Private data release via bayesian networks.” *ACM Transactions on Database Systems (TODS)* 42.4 (2017), pp. 1–41.
- [51] Zhikun Zhang, Tianhao Wang, Ninghui Li, Jean Honorio, Michael Backes, Shibo He, Jiming Chen, and Yang Zhang. “Privsyn: Differentially private data synthesis.” *30th {USENIX} Security Symposium ({USENIX} Security 21)*. 2021.
- [52] T. Zhu, G. Li, W. Zhou, and P. S. Yu. “Differentially Private Data Publishing and Analysis: A Survey.” *IEEE Transactions on Knowledge and Data Engineering* 29.8 (Aug. 2017), pp. 1619–1638.
- [53] T. Zhu, G. Li, W. Zhou, and P. S. Yu. “Differentially Private Data Publishing and Analysis: A Survey.” *IEEE Transactions on Knowledge and Data Engineering* 29.8 (Aug. 2017), pp. 1619–1638.

## A Proof of Prop. 4.1 when using only the first moment of PFs

*Proof.* Let  $\mathbf{n}$  denote the noise added to the mean embedding: for Prop. 4.1, this is simply  $\boldsymbol{\eta}_1$  of eq. 6, but the following section will make it more generic. Thus, we have that

$$\begin{aligned}
& \mathbb{E}_{\mathbf{n}} \left[ \left| \widetilde{\text{MMD}}_{k_{\Phi}}^2(P, Q) - \text{MMD}_{k_{\Phi}}^2(P, Q) \right| \right], \\
&= \mathbb{E}_{\mathbf{n}} \left[ \left| \|\boldsymbol{\mu}_P(\mathcal{D}) + \mathbf{n} - \boldsymbol{\mu}_{Q_{g_{\theta}}}(\tilde{\mathcal{D}})\|^2 - \|\boldsymbol{\mu}_P(\mathcal{D}) - \boldsymbol{\mu}_{Q_{g_{\theta}}}(\tilde{\mathcal{D}})\|^2 \right| \right], \\
&= \mathbb{E}_{\mathbf{n}} \left[ \left| \mathbf{n}^{\top} \mathbf{n} + 2\mathbf{n}^{\top} (\boldsymbol{\mu}_P(\mathcal{D}) - \boldsymbol{\mu}_{Q_{g_{\theta}}}(\tilde{\mathcal{D}})) \right| \right] \\
&\leq \mathbb{E}_{\mathbf{n}} [\mathbf{n}^{\top} \mathbf{n}] + 2 \mathbb{E}_{\mathbf{n}} \left[ \left| \mathbf{n}^{\top} (\boldsymbol{\mu}_P(\mathcal{D}) - \boldsymbol{\mu}_{Q_{g_{\theta}}}(\tilde{\mathcal{D}})) \right| \right], \tag{9}
\end{aligned}$$

by rearranging the definitions given in eq. 3 and eq. 4 and using the triangle inequality.

Now, when we use only first-moment features, we know the value of  $\mathbf{n} \sim \mathcal{N}(0, \sigma^2 (\frac{2C}{m})^2 I)$ ; thus we know  $\mathbb{E}_{\mathbf{n}} \mathbf{n}^{\top} \mathbf{n} = \text{Tr}(\mathbb{E}_{\mathbf{n}} \mathbf{n} \mathbf{n}^{\top}) = \sigma^2 (\frac{2C}{m})^2 D$ . For the other term, we have that

$$(\boldsymbol{\mu}_P(\mathcal{D}) - \boldsymbol{\mu}_{Q_{g_{\theta}}}(\tilde{\mathcal{D}}))^{\top} \mathbf{n} \sim \mathcal{N}\left(0, \sigma^2 \left(\frac{2C}{m}\right)^2 \|\boldsymbol{\mu}_P(\mathcal{D}) - \boldsymbol{\mu}_{Q_{g_{\theta}}}(\tilde{\mathcal{D}})\|^2\right),$$

and so its absolute value follows a scaled chi distribution with one degree of freedom. The mean of a  $\chi(1)$  distribution is  $\frac{\sqrt{2} \Gamma(1)}{\Gamma(1/2)} = \sqrt{\frac{2}{\pi}}$ ; thus we have

$$\mathbb{E}_{\mathbf{n}} \left[ \left| \widetilde{\text{MMD}}_{k_{\Phi}}^2(P, Q) - \text{MMD}_{k_{\Phi}}^2(P, Q) \right| \right] \leq \frac{4D\sigma^2 C^2}{m^2} + \frac{4\sqrt{2}\sigma C}{m\sqrt{\pi}} \|\boldsymbol{\mu}_P(\mathcal{D}) - \boldsymbol{\mu}_{Q_{g_{\theta}}}(\tilde{\mathcal{D}})\|_2.$$

The desired result follows by recalling the definition of the MMD in eq. 1.  $\square$

## B More generic version of Prop. 4.1

We will now give a version of Prop. 4.1 for arbitrary noise structures, which in particular will also apply to the case where we use both first- and second-moment features.

**Proposition B.1.** *Given datasets  $\mathcal{D} = \{\mathbf{x}_i\}_{i=1}^m$  and  $\tilde{\mathcal{D}} = \{\tilde{\mathbf{x}}_j\}_{j=1}^n$ , let  $\mathbf{a} = \boldsymbol{\mu}_P(\mathcal{D}) - \boldsymbol{\mu}_{Q_{g_{\theta}}}(\tilde{\mathcal{D}})$ , and define  $\widetilde{\text{MMD}}_{k_{\Phi}}^2(\mathcal{D}, \tilde{\mathcal{D}}) = \|\mathbf{a} + \mathbf{n}\|^2$  for a noise vector  $\mathbf{n} \sim \mathcal{N}(0, \Sigma)$ . Introducing the noise  $\mathbf{n}$  affects the expected absolute error as*

$$\mathbb{E}_{\mathbf{n}} \left[ \left| \widetilde{\text{MMD}}_{k_{\Phi}}^2(\mathcal{D}, \tilde{\mathcal{D}}) - \text{MMD}_{k_{\Phi}}^2(\mathcal{D}, \tilde{\mathcal{D}}) \right| \right] \leq \text{Tr}(\Sigma) + \sqrt{\frac{2}{\pi} \mathbf{a}^{\top} \Sigma \mathbf{a}}. \tag{10}$$

*Proof.* The proof is essentially identical to the previous one. From eq. 9, we handle the first term as

$$\mathbb{E} \mathbf{n}^{\top} \mathbf{n} = \text{Tr}(\mathbb{E} \mathbf{n} \mathbf{n}^{\top}) = \text{Tr}(\Sigma),$$

and the second is based on

$$\mathbf{a}^{\top} \mathbf{n} \sim \mathcal{N}(0, \mathbf{a}^{\top} \Sigma \mathbf{a})$$

giving that

$$\mathbb{E} |\mathbf{a}^{\top} \mathbf{n}| = \sqrt{\frac{2}{\pi} \mathbf{a}^{\top} \Sigma \mathbf{a}}.$$

$\square$

Applying this to the case where we use both first- and second-moment features, we have that

$$\Sigma = \begin{bmatrix} \sigma^2 \left(\frac{2C_1}{m}\right)^2 I_D & 0 \\ 0 & \sigma^2 \left(\frac{2C_2}{m}\right)^2 I_D \end{bmatrix} = \frac{4\sigma^2}{m^2} \begin{bmatrix} C_1^2 I_D & 0 \\ 0 & C_2^2 I_D \end{bmatrix},$$

giving

$$\text{Tr}(\Sigma) = \frac{4D\sigma^2}{m^2}(C_1^2 + C_2^2)$$

and

$$\mathbf{a}^\top \Sigma \mathbf{a} = \frac{4\sigma^2}{m^2} \left[ C_1^2 \|\boldsymbol{\mu}_P^{\phi_1}(\mathcal{D}) - \boldsymbol{\mu}_{Q_{g_\theta}}^{\phi_1}(\tilde{\mathcal{D}})\|_2^2 + C_2^2 \|\boldsymbol{\mu}_P^{\phi_2}(\mathcal{D}) - \boldsymbol{\mu}_{Q_{g_\theta}}^{\phi_2}(\tilde{\mathcal{D}})\|_2^2 \right].$$

## C Proof of Prop. 4.2 when using first moment of PFs

We will prove a more generic version as in the previous section, then show that Prop. 4.2 is a special case.

**Proposition C.1.** *Given datasets  $\mathcal{D} = \{\mathbf{x}_i\}_{i=1}^m$  and  $\tilde{\mathcal{D}} = \{\tilde{\mathbf{x}}_j\}_{j=1}^n$ , let  $\mathbf{a} = \mu_P(\mathcal{D}) - \mu_{Q_{g_\theta}}(\tilde{\mathcal{D}})$ , and define  $\widetilde{\text{MMD}}_{k_\Phi}^2(\mathcal{D}, \tilde{\mathcal{D}}) = \|\mathbf{a} + \mathbf{n}\|_2^2$  for a noise vector  $\mathbf{n} \sim \mathcal{N}(0, \Sigma)$ . Then it holds with probability at least  $1 - \rho$  that*

$$\begin{aligned} & \left| \widetilde{\text{MMD}}_{k_\Phi}^2(P, Q) - \text{MMD}_{k_\Phi}^2(P, Q) \right| \\ & \leq \text{Tr}(\Sigma) + \sqrt{\frac{2}{\pi}} \|\Sigma^{\frac{1}{2}} \mathbf{a}\|_2 + \left( 2\|\Sigma\|_F + \sqrt{2}\|\Sigma^{\frac{1}{2}} \mathbf{a}\|_2 \right) \sqrt{\log(\frac{2}{\rho})} + 2\|\Sigma\|_{op} \log(\frac{2}{\rho}). \end{aligned} \quad (11)$$

*Proof.* We have, as in the equations leading up to eq. 9, that

$$\left| \widetilde{\text{MMD}}_{k_\Phi}^2(P, Q) - \text{MMD}_{k_\Phi}^2(P, Q) \right| = \left| \mathbf{n}^\top \mathbf{n} + 2\mathbf{n}^\top \mathbf{a} \right| \leq \mathbf{n}^\top \mathbf{n} + 2\left| \mathbf{n}^\top \mathbf{a} \right|.$$

Let  $\mathbf{z} \sim \mathcal{N}(0, I)$  be such that  $\mathbf{n} = \Sigma^{\frac{1}{2}} \mathbf{z}$ . We will now bound each term separately.

First, denoting the eigendecomposition of  $\Sigma$  as  $\mathbf{Q}\mathbf{\Lambda}\mathbf{Q}^\top$ , we can write

$$\mathbf{n}^\top \mathbf{n} = (\mathbf{Q}^\top \mathbf{z})^\top \mathbf{\Lambda} (\mathbf{Q}^\top \mathbf{z}),$$

in which  $\mathbf{Q}^\top \mathbf{z} \sim \mathcal{N}(0, I)$  and  $\mathbf{\Lambda}$  is diagonal. Thus, applying Lemma 1 of Laurent and Massart [21], we obtain that with probability at least  $1 - \frac{\rho}{2}$ ,

$$\|\mathbf{n}\|_2^2 \leq \text{Tr}(\Sigma) + 2\|\Sigma\|_F \sqrt{\log(\frac{2}{\rho})} + 2\|\Sigma\|_{op} \log(\frac{2}{\rho}). \quad (12)$$

We can write the second term as  $\mathbf{a}^\top \mathbf{n} = \mathbf{a}^\top \Sigma^{\frac{1}{2}} \mathbf{z}$ , which is a function of a standard normal variable with Lipschitz constant  $\|\Sigma^{\frac{1}{2}} \mathbf{a}\|_2$ . Thus, applying the standard Gaussian Lipschitz concentration inequality [3, Theorem 5.6], we obtain that with probability at least  $1 - \frac{\rho}{2}$ ,

$$\left| \mathbf{z}^\top \Sigma^{\frac{1}{2}} \mathbf{a} \right| - \mathbb{E} \left| \mathbf{z}^\top \Sigma^{\frac{1}{2}} \mathbf{a} \right| \leq \|\Sigma^{\frac{1}{2}} \mathbf{a}\|_2 \sqrt{2 \log(\frac{2}{\rho})}.$$

Since  $\mathbb{E} \left| \mathbf{z}^\top \Sigma^{\frac{1}{2}} \mathbf{a} \right| = \|\Sigma^{\frac{1}{2}} \mathbf{a}\|_2 \sqrt{\frac{2}{\pi}}$ , this is equivalent to saying that

$$\left| \mathbf{n}^\top \mathbf{a} \right| \leq \|\Sigma^{\frac{1}{2}} \mathbf{a}\|_2 \left( \sqrt{\frac{2}{\pi}} + \sqrt{2 \log(\frac{2}{\rho})} \right). \quad (13)$$

The final statement follows by combining eq. 12 and eq. 13 with a union bound.  $\square$

Prop. 4.2 follows from plugging in  $\Sigma = \frac{4C^2\sigma^2}{m^2} I_D$  into Prop. C.1, in which case we have  $\text{Tr}(\Sigma) = \frac{4C^2\sigma^2}{m^2} D$ ,  $\|\Sigma^{\frac{1}{2}} \mathbf{a}\|_2 = \frac{2C\sigma}{m} \text{MMD}_{k_\Phi}(\mathcal{D}, \tilde{\mathcal{D}})$ ,  $\|\Sigma\|_F = \frac{4C^2\sigma^2}{m^2} \sqrt{D}$ , and  $\|\Sigma\|_{op} = \frac{4C^2\sigma^2}{m^2}$ .

For first- and second-moment features, we have  $\|\Sigma^{\frac{1}{2}} \mathbf{a}\|_2 = \sqrt{\mathbf{a}^\top \Sigma \mathbf{a}}$  from above, while  $\|\Sigma\|_F = \frac{4\sigma^2\sqrt{D}}{m^2}(C_1^2 + C_2^2)$  and  $\|\Sigma\|_{op} = \frac{4\sigma^2}{m^2} \max(C_1^2, C_2^2)$ .

## D Extended Implementation details

**Repository.** Our anonymized code is available at <https://anonymous.4open.science/r/dp-mepf>; the readme files contain further instructions on how to run the code.

### D.1 Hyperparameter settings

For each dataset, we tune the generator learning rate ( $\text{LR}_{gen}$ ) and moving average learning rate ( $\text{LR}_{avg}$ ) from choices  $10^{-k}$  with  $k \in \{2, 3, 4, 5, 6\}$  once for the non-private setting and once at  $\epsilon = 2$ . The latter is used in all private experiments for that dataset, as shown in 6. After some initial unstructured experimentation, hyperparameters are chosen with identical values across dataset shown in 7

For the Cifar10 DP-MERF baseline we tested random tuned random features dimension  $d \in \{10000, 50000\}$ , random features sampling distribution  $\sigma \in \{100, 300, 1000\}$ , learning rate decay by 10% every  $e \in \{1000, 10000\}$  iterations and learning rate  $10^{-k}$  with  $k \in \{2, 3, 4, 5, 6\}$ . Results presented use  $d = 500000, \sigma = 1000, e = 10000, k = 3$ .

Table 6: Learning rate hyperparameters across datasets

	$\text{LR}_{gen}$	$\text{LR}_{avg}$
MNIST-nonDP	$10^{-5}$	$10^{-3}$
MNIST-DP	$10^{-5}$	$10^{-4}$
FashionMNIST-nonDP	$10^{-5}$	$10^{-3}$
FashionMNIST-DP	$10^{-4}$	$10^{-3}$
CelebA-nonDP	$10^{-3}$	$10^{-4}$
CelebA-DP	$10^{-3}$	$10^{-4}$
Cifar10-nonDP labeled	$10^{-3}$	$10^{-3}$
Cifar10-DP labeled	$10^{-5}$	$10^{-5}$
Cifar10-nonDP unlabeled	$10^{-4}$	$10^{-3}$
Cifar10-DP unlabeled	$10^{-5}$	$10^{-4}$

Table 7: Hyperparameters fixed across datasets

Parameter	Value
$(\phi_1)$ -bound	1
$(\phi_2)$ -bound	1
iterations	100,000
batch size Cifar10 and CelebA	64
batch size MNIST and FashionMNIST	100
seeds	1,2,3

## E Detailed Tables

Below we present the results from the main paper with added  $a \pm b$  notation, where  $a$  is the mean and  $b$  is the standard deviation of the score distribution across three independent runs.

Table 8: Downstream accuracies of our method for MNIST at varying values of  $\epsilon$

		$\epsilon = \infty$	$\epsilon = 10$	$\epsilon = 5$	$\epsilon = 2$	$\epsilon = 1$	$\epsilon = 0.2$
MLP	DP-MEPF $(\phi_1, \phi_2)$	$91.4 \pm 0.3$	$89.8 \pm 0.5$	$89.9 \pm 0.2$	$89.3 \pm 0.3$	$89.3 \pm 0.6$	$79.9 \pm 1.3$
	DP-MEPF $(\phi_1)$	$88.2 \pm 0.6$	$88.8 \pm 0.1$	$88.4 \pm 0.5$	$88.0 \pm 0.2$	$87.5 \pm 0.6$	$77.1 \pm 0.4$
LogReg	DP-MEPF $(\phi_1, \phi_2)$	$84.6 \pm 0.5$	$83.4 \pm 0.6$	$83.3 \pm 0.7$	$82.9 \pm 0.7$	$82.5 \pm 0.5$	$75.8 \pm 1.1$
	DP-MEPF $(\phi_1)$	$81.4 \pm 0.4$	$80.8 \pm 0.9$	$80.8 \pm 0.8$	$80.5 \pm 0.6$	$79.0 \pm 0.6$	$72.1 \pm 1.4$

Table 9: Downstream accuracies of our method for FashionMNIST at varying values of  $\epsilon$

		$\epsilon = \infty$	$\epsilon = 10$	$\epsilon = 5$	$\epsilon = 2$	$\epsilon = 1$	$\epsilon = 0.2$
MLP	DP-MEPF ( $\phi_1, \phi_2$ )	$74.4 \pm 0.3$	$76.0 \pm 0.4$	$75.8 \pm 0.6$	$75.1 \pm 0.3$	$74.7 \pm 1.1$	$70.4 \pm 1.9$
	DP-MEPF ( $\phi_1$ )	$73.8 \pm 0.5$	$75.5 \pm 0.6$	$75.1 \pm 0.8$	$75.8 \pm 0.7$	$75.0 \pm 1.8$	$69.0 \pm 1.5$
LogReg	DP-MEPF ( $\phi_1, \phi_2$ )	$74.3 \pm 0.1$	$75.7 \pm 1.0$	$75.2 \pm 0.4$	$75.8 \pm 0.4$	$75.4 \pm 1.1$	$72.5 \pm 1.2$
	DP-MEPF ( $\phi_1$ )	$72.8 \pm 0.5$	$75.5 \pm 0.1$	$75.5 \pm 0.8$	$76.4 \pm 0.8$	$76.2 \pm 0.8$	$71.7 \pm 0.4$

Table 10: CelebA FID scores (lower is better)

	$\epsilon = \infty$	$\epsilon = 10$	$\epsilon = 5$	$\epsilon = 2$	$\epsilon = 1$	$\epsilon = 0.2$
DP-MEPF ( $\phi_1, \phi_2$ )	$24.53 \pm 2.02$	$25.84 \pm 1.16$	$24.14 \pm 0.35$	$25.51 \pm 1.38$	$23.28 \pm 0.66$	$42.44 \pm 0.38$
DP-MEPF ( $\phi_1$ )	$23.35 \pm 1.33$	$23.77 \pm 2.44$	$22.79 \pm 0.71$	$26.02 \pm 1.70$	$25.41 \pm 2.85$	$46.55 \pm 3.67$

Table 11: FID scores for synthetic *labelled* CIFAR-10 data (generating both labels and input images)

	$\epsilon = \infty$	$\epsilon = 10$	$\epsilon = 5$	$\epsilon = 2$	$\epsilon = 1$	$\epsilon = 0.2$
<b>DP-MEPF</b> ( $\phi_1, \phi_2$ )	$45.2 \pm 8.2$	$85 \pm 1.2$	$83 \pm 1.3$	$92 \pm 1.0$	$103 \pm 4.7$	$367 \pm 22.2$
<b>DP-MEPF</b> ( $\phi_1$ )	$45.2 \pm 7.7$	$90 \pm 0.9$	$91 \pm 0.6$	$95 \pm 4.0$	$114 \pm 6.7$	$491 \pm 5.1$
DP-MERF	$127.4 \pm 1.8$	$124.4 \pm 2.3$	$124.0 \pm 0.8$	$126.5 \pm 2.8$	$122.7 \pm 1.1$	$412.8 \pm 0.8$

Table 12: Test accuracies (higher better) of ResNet9 trained on CIFAR-10 synthetic data with varying privacy guarantees. When trained on real data, test accuracy is 88.3%

	$\epsilon = \infty$	$\epsilon = 10$	$\epsilon = 5$	$\epsilon = 2$	$\epsilon = 1$	$\epsilon = 0.2$
<b>DP-MEPF</b> ( $\phi_1$ )	$54.9 \pm 5.4$	$52.4 \pm 0.9$	$49.9 \pm 1.8$	$47.6 \pm 1.8$	$32.8 \pm 0.9$	$10.2 \pm 0.1$
<b>DP-MEPF</b> ( $\phi_1, \phi_2$ )	$54.0 \pm 0.8$	$54.4 \pm 0.5$	$50.1 \pm 2.4$	$45.8 \pm 1.4$	$34.9 \pm 0.8$	$11.8 \pm 0.9$
DP-MERF	$13.2 \pm 0.4$	$13.4 \pm 0.4$	$13.5 \pm 0.5$	$13.8 \pm 1.4$	$13.1 \pm 0.7$	$10.4 \pm 0.5$

Table 13: FID scores for synthetic *unlabelled* CIFAR-10 data

	$\epsilon = \infty$	$\epsilon = 5$	$\epsilon = 2$	$\epsilon = 1$
<b>DP-MEPF</b> ( $\phi_1, \phi_2$ )	$44.9 \pm 2.0$	$51.4 \pm 1.3$	$54.5 \pm 1.5$	$64.3 \pm 1.0$
<b>DP-MEPF</b> ( $\phi_1$ )	$38.9 \pm 1.3$	$48.7 \pm 0.6$	$51.9 \pm 1.9$	$63.8 \pm 1.5$



## F Additional Plots

Below we show samples from our generated MNIST and FashionMNIST data in Fig. 5 and Fig. 6 respectively.

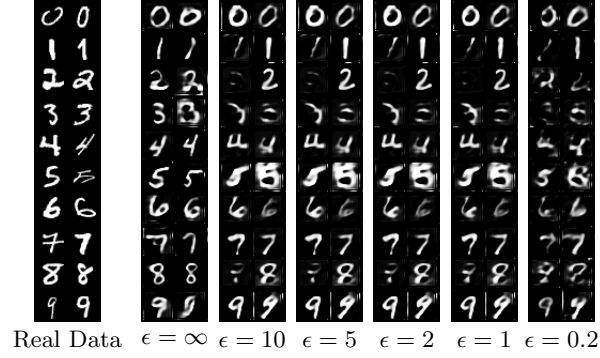


Figure 5: MNIST samples produced with DP-MEPF ( $\phi_1, \phi_2$ ) at various levels of privacy

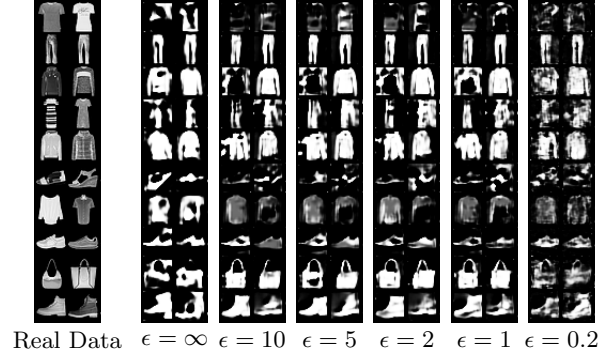


Figure 6: Fashion-MNIST samples produced with DP-MEPF ( $\phi_1, \phi_2$ ) at various levels of privacy